ИЗСЛЕДВАНЕ НА МНОГОФАЗНИ ИЗТОЧНИЦИ НА ТОК ЗА ЗАРЯДНИ СТАНЦИИ

INVESTIGATION OF MULTIPHASE CURRENT SOURCES FOR CHARGING STATIONS

Stoyan Vuchev[1], Dimitar Arnaudov[1]
[1] *Technical University of Sofia, Bulgaria*
stoyan.vuchev@tu-sofia.bg, dda@tu-sofia.bg

Abstract

The paper presents investigation of two multiphase current source topologies for charging applications in energy storage systems. The current sources consist of identical modules with different connections between each other. The modules are realized on the base of resonant converters and rectifiers. Using different system topologies, different modular multiphase current sources with specific characteristics are obtained. The paper points advantages and disadvantages of the two examined topologies. Simulation models are developed in LTspice for the investigation purposes. The asymmetric operation, the ripple, the output current control options and the efficiency of the two converters are compared. The stresses over the passive and the semiconductor components are discussed, including considerations for the circuit design.

Keywords: Charging Stations, Current-Driven Converter, Multiphase Topology.

INTRODUCTION

Current-driven topologies based on resonant power converters [1, 2] are often used for charging applications due to their high overall efficiency and ability to provide different operating modes throughout the charging process. Such converter systems are often realized on a modular principle with several modules operating to a common load [1, 2, 3] in order to provide higher output power and reliability.

As a result of the circuit components tolerances, asymmetry in the topology operation may occur depending on the interactions between the individual modules [2]. The type of connection between the modules may either facilitate or prevent from such events.

The following paper presents results from investigation of two current-driven topologies suitable for charging applications. Modelling and simulation examination of the converters is performed in the environment of LTspice. On the base of the obtained results, comparison between the two systems is made. The advantages and disadvantages are discussed considering the interference between the individual modules during operation, as well as, the whole topology behavior with respect to the load.

EXAMINED CHARGING CONVERTER TOPOLOGIES

Fig. 1 and Fig. 2 present block diagrams of the two investigated current source topologies. The modules used for the realization of the two systems are based on half-bridge series resonant inverters with voltage limitation applied to part of the resonant tank capacitor [4, 5, 6]. Each of them is supplied by an individual controllable rectifier [4].

The first examined topology, conditionally designated as **Topology I**, consists of N number of modules supplying a single multiphase rectifier.

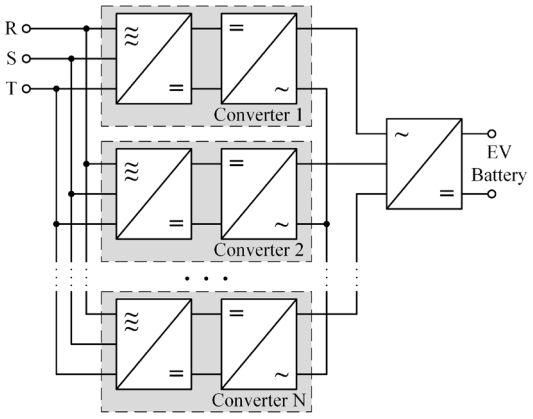

***Fig. 1**. Block diagram of a topology based on a single multiphase output rectifier (**Topology I**).*

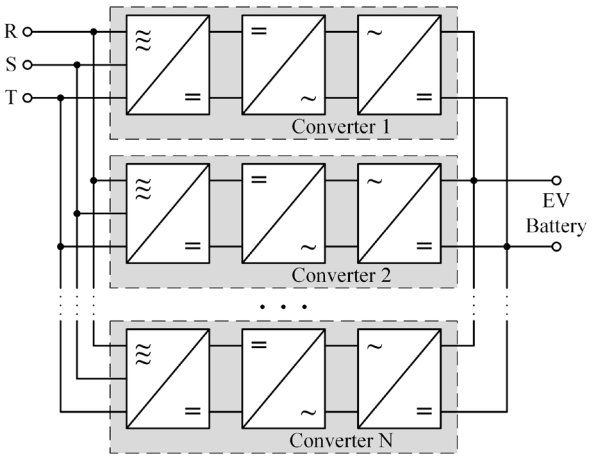

***Fig. 2**. Block diagram of a topology based on multiple single-phase rectifiers connected in parallel to the common load (**Topology II**).*

Contrariwise, the second converter system, conditionally designated as **Topology II**, consists again of N number of modules each of them connected to an individual single-phase rectifier. The rectifiers are furtherly connected in parallel to the common load.

Fig. 3 presents the particular circuit used for realization of the **Topology I** output multiphase rectifier. As the resonant converter modules behave as ideal current sources, the rectifier is considered to operate as a current-driven. A detailed mathematical analysis of the output current waveforms and values for the particular case of a three-phase current-driven rectifier is presented in [2] for both symmetric and asymmetric operation.

Fig. 4 presents the particular circuit used for realization of the **Topology II** output. Analogically, the multiple single-phase rectifiers can be considered as current-driven. Analysis of the operation of such class D bridge rectifiers is presented in [7].

In both topologies, transformers are placed between the resonant inverter stage and the output rectifiers for galvanic isolation [4].

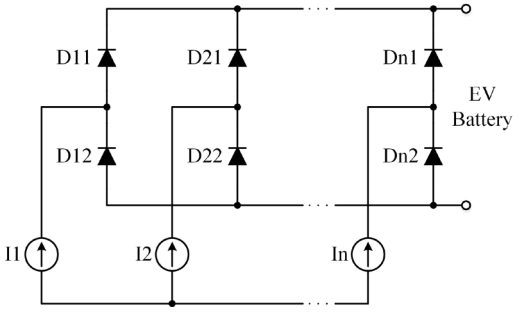

***Fig. 3**. Circuit of the single multiphase rectifier topology (**Topology I**).*

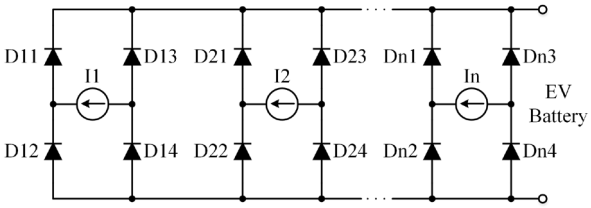

***Fig. 4**. Circuit of the multiple single-phase rectifiers topology (**Topology II**).*

In order to obtain high overall efficiency, both topologies may be realized with synchronous rectifier circuits [8].

MODELLING AND SIMULATION INVESTIGATIONS

Models of the two converter systems are developed in the software environment of LTspice in accordance with the presented in Fig. 1 to Fig. 4 circuits. For the purposes of the following investigation, balanced three-phase topologies with modules phase shifted at 120 degrees are used in order to provide symmetric operation. The input rectifiers are substituted with ideal DC voltage sources with a value of 300V. The resonant inverters circuitry is presented in [4]. Transformers with a unity ratio are used.

Computer simulations of the two converter topologies operation during charging of energy storage element (ESE) are performed. Identical load parameters are applied for the two circuits. The initial ESE voltage is 100V. Its capacity is significantly reduced in order to optimize the time of the simulation process. The resonant inverters are operated at 100kHz.

Fig. 5 presents transistor current waveforms for a single inverter stage supplying the load via a single-phase rectifier (as in **Topology II**). Operation above the resonant frequency can be obtained. The maximum forward and reverse current values and the interval of conduction of the reverse diode are presented in Table 1.

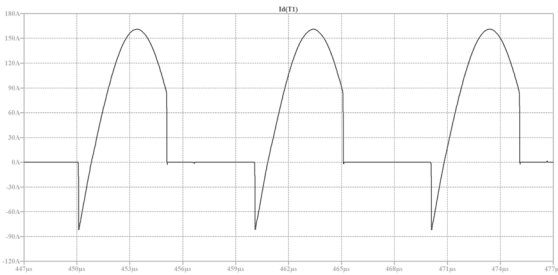

***Fig. 5**. Waveforms of the transistor current in one of the resonant inverter stages operating alone with a single-phase rectifier.*

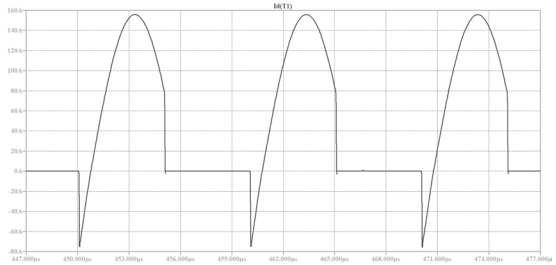

***Fig. 6**. Waveforms of the transistor current in one of the resonant inverter stages during simultaneous operation of three stages with single-phase rectifiers (**Topology II**).*

Fig. 6 presents identical waveforms corresponding to the operation of all the three **Topology II** modules to the common load. From the presented in Table 1 values for the maximum forward and reverse current values and the interval of conduction of the reverse diode, it can be seen that the stages do not interact during simultaneous operation. The observed negligible difference between the values in the two cases is due to the parasitic voltage drop in the load connections. This voltage drop is current dependent and influences on the resultant anti-emf voltage applied to each of the modules individually.

Fig. 7 presents transistor current waveforms for a single inverter stage supplying the load via a multiphase rectifier (as in **Topology I**). The presented in Table 1 values negligibly defer from those for the **Topology II** single module due to the two rectifiers specificities.

Fig. 8 presents transistor current waveforms corresponding to the operation of all the three **Topology I** modules to the common load. From the presented in Table 1 values, a significant difference can be seen. Due to the interaction between the modules in this case, the resultant anti-emf voltage is distributed between them resulting in variation of the operating mode.

***Table. 1**. Maximum forward and reverse transistor current values and reverse diode interval of conduction.*

Parameter	Topology I		Topology II	
	1 module	3 modules	1 module	3 modules
Maximum Forward Current	160.939A	216.05A	162.25A	156.02A
Maximum Reverse Current	67.518A	182.82A	82.37A	74.60A
Reverse Diode Conduction Time	705.157ns	1.573µs	761.589ns	729.685ns

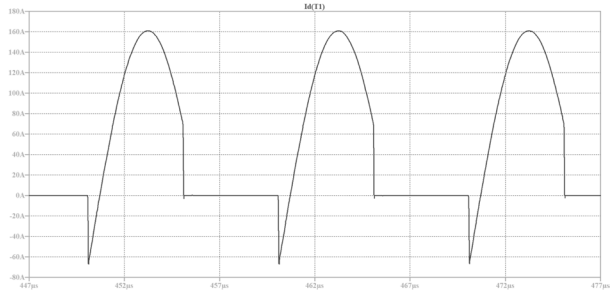

***Fig. 7**. Waveforms of the transistor current in one of the resonant inverter stages operating alone with a multiphase rectifier (**Topology I**).*

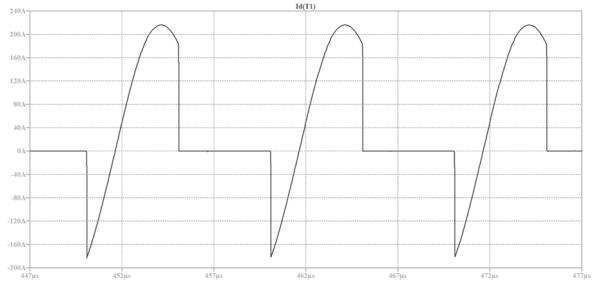

***Fig. 8**. Waveforms of the transistor current in one of the resonant inverter stages during simultaneous operation of three stages with a multiphase rectifier (**Topology I**).*

From Table 1 and Fig. 5 to Fig. 8, it can be seen that the current stress of the **Topology I** resonant inverters transistors significantly increases compared to that of **Topology II**, which is due to the different operating mode – more energy is consumed and then returned back to the supply source.

Comparison between the two topologies current stresses can also be made with respect to the output rectifiers. Fig. 9 and Fig. 10 present waveforms of the two converter systems output currents and rectifiers diodes currents respectively. From the presented in Table 2 values of the maximum diode currents, it can be seen that the **Topology I** devices suffer more current stress. Moreover, the average value of the charging current is significantly lower compared to that of **Topology II**, which is due to the different operating modes.

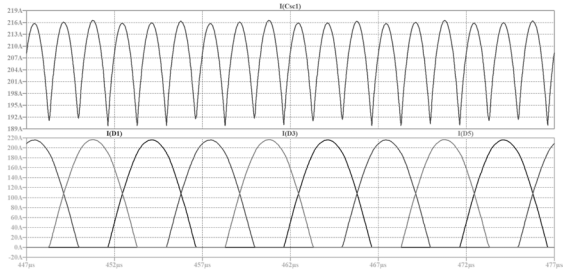

***Fig. 9**. Waveforms of the **Topology I** output current and the multiphase rectifier diodes currents.*

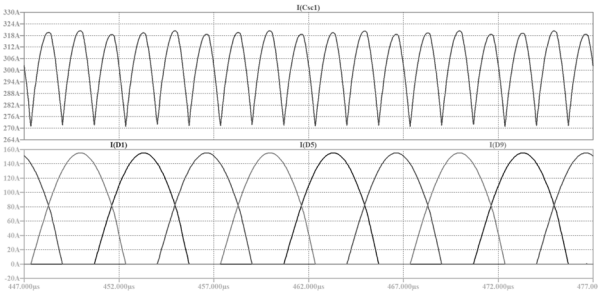

***Fig. 10**. Waveforms of the **Topology II** output current and the single-phase rectifiers diodes currents.*

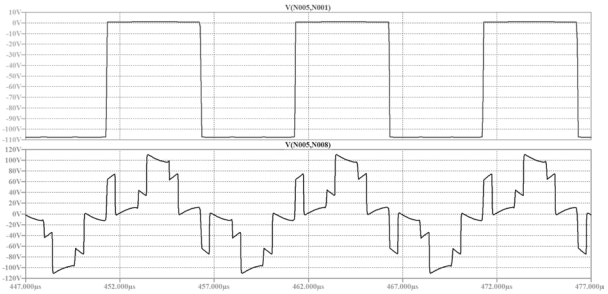

***Fig. 11**. Waveforms of the rectifier diode reverse voltage and the transformer secondary coil voltage **(Topology I)**.*

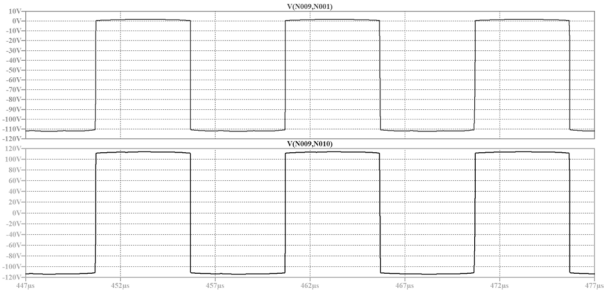

***Fig. 12**. Waveforms of the rectifier diode reverse voltage and the transformer secondary coil voltage **(Topology II)**.*

The reduction of the current stress applied to the **Topology II** rectifiers diodes is also due to the doubled number of devices and the current sharing between them. Thus, all the three modules can simultaneously operate as current sources, whereas only two **Topology I** stages can operate as current sources with the remaining one operating as a current sink [2]. Still, the increased number of rectifier switches is a disadvantage resulting in increased system cost and lower overall efficiency.

Another drawback of Topology II compared to **Topology I** is the output current ripple. Table 2 presents the two values calculated in accordance with the presented in [2] expression. The simulation results slightly vary from the theoretical as the corresponding currents are measured with the software environment cursor. Moreover, models of real semiconductor devices are used. For both of the topologies, however, an additional output filter may be necessary in order to meet the charging current ripple requirements.

Table 2 also presents results for the maximum reverse voltage ratings of the two topologies rectifier diodes. For both of the converter systems, the values are similar and correspond to the anti-emf voltage of the load. Fig. 11 and Fig. 12 present waveforms of these reverse diode voltages.

***Table. 2**. Maximum rectifiers current and voltage ratings and charging currents parameters.*

Parameter	Topology I 3 modules	Topology II 3 modules
Rectifier Diode Maximum Current	201.22A	154.641A
Rectifier Diode Maximum Reverse Voltage	107.511V	111.738V
Average Charging Current	207.3A	302.45A
Charging Current Ripple	6.39%	8.07%

Fig. 11 and Fig. 12 also present waveforms of the two topologies transformers secondary coils voltages. Both voltage waveforms correspond to the anti-emf voltage applied to the corresponding resonant converter module.

In **Topology I**, this voltage depends on the rectifier operating specificities [2]. In this case, the wye connection of the transformers secondary coils is responsible for the anti-emf voltage distribution among the individual modules, which explains the complicated shape of the observed waveforms.

In **Topology II**, each of the resonant converter stages operates independently as the output single-phase rectifiers only share the common load current. As a result, the whole anti-emf voltage is applied to the corresponding transformer secondary coil. Due to the specificities of the single-phase rectifier [7], it has a rectangular shape.

CONCLUSION

The following paper presents results from examination of the operating specificities of two current source converter topologies suitable for charging applications. Modelling and investigation of the systems behavior is done in the software environment of LTspice. Analysis of the output rectifiers current and

voltage stresses is performed. Based on the obtained simulation results, considerations are made for the output parameters and the overall efficiency of the converters.

Due to the interaction between the individual modules of **Topology I** during operation, different operating mode is obtained for the same load compared to the one of the single operating stages, as well as, to the whole **Topology II** system one. As a result, significant current stress is applied to the resonant inverters transistors and the output rectifier diodes. Moreover, this stress is also applied to the passive components of the corresponding resonant tanks. On the contrary, such event is not observed with **Topology II** as the interaction between its modules is negligible – they only share the charging current.

Increase in the voltage stress is not observed with any of the two examined topologies. The maximum reverse voltage of the rectifiers devices depends only on the anti-emf voltage applied by the load.

However, the interaction between the **Topology I** modules can be observed from the presented waveforms of the transformers secondary coils voltages. Due to the specific connection between these coils, the load anti-emf voltage is distributed depending on the specific interval of operation of each inverter stage throughout the switching frequency period. As a result, complicated shapes of the applied resultant voltage are observed, which may result in additional transformer losses. Such event is again not observed with **Topology II** where the shape of the applied voltages is rectangular.

Advantages of **Topology I** are the lower output current ripple and the optimized number of rectifier switching devices. The second fact should also be considered with respect to the overall efficiency and the cost of the two examined systems. However, both the two converter topologies may need additional filtering of the output current in order to meet the specific requirements for the particular charging process. Moreover, the overall efficiency of the two may be significantly improved by the implementation of synchronous output rectifier stages.

Considering the advantages and disadvantages of the two converter systems, **Topology II** appears to be more favorable for high-voltage high-power applications such as charging of energy storage elements and electric vehicle fast charging stations. This topology is also more suitable for modular realization as the interaction between the individual stages during operation is negligible.

ACKNOWLEDGEMENT

The research is carried out within the framework of the “Electronic converters for electric vehicle charging stations” project, contract 182ПД0012-03, Scientific and Research Sector at the Technical University of Sofia.

REFERENCE

[1] Sun, L., Y. Chen, X. Xia, L. Peng, Y. Kang, Design and optimization of parallel DC-DC system based on current-driven phase shift full bridge converter, 29th Annual IEEE Applied Power Electronics Conference and Exposition (APEC), 2014, ISSN: 1048-2334, pp. 2048-2053.

[2] Arnaudov, D., S. Vuchev, Modelling and Investigation of Multi-Phase Rectifiers Supplied by Resonant Converters, Proceedings of ISSE 2018, ISBN: 978-1-5386-5731-7, DOI: 10.1109/ISSE.2018.8443760.

[3] Chub, A., O. Husev, D. Vinnikov, Input-Parallel Output-Series Connection of Isolated Quasi-Z-Source DC-DC Converters, Electric Power Quality and Supply Reliability Conference (PQ), June 11-13, 2014, pp. 277-284.

[4] Vuchev, S., D. Arnaudov, D. Penev, N. Hinov, Modeling and Investigation of Converter Modules Simultaneous Operation in Electric Vehicle Charging Systems, Proceedings of PCIM Europe 2018, ISBN: 978-3-8007-4646-0.

[5] Agraval, J., S. Kim, C. Lee, Capacitor voltage clamped series resonant power supply with improved cross regulation, 1989 IEEE Industry Applications Society Annual Meeting, vol. 1, pp. 1141-1146.

[6] Madzharov, N., Autonomous inverters with energy dosing for ultrasonic application, Proceedings of ICEST 2013, vol. 2, pp.647-651.

[7] Kazimierczuk, M., K., D. Czarkowski, Resonant Power Converters, Second Edition, John Wiley & Sons, Inc., 2011.

[8] Ma, Y., X. Xie, Z. Qian, Frequency-Controlled LCC Resonant Converter with Synchronous Rectifier, Proceedings of PEDS 2007, ISSN: 2164-5264, pp. 1442-1445.